Applied Radiation and Isotopes

Monte Carlo Verification of Output Correction Factors for a TrueBeam STx linac

--Manuscript Draft--

Manuscript Number:	ARI_2019_1005R3
Article Type:	Full Length Article
Section/Category:	Radiation Sources and Applications
Keywords:	output correction factors; VMAT; small field dosimetry; IMRT; Computational dosimetry; monte carlo simulation; Stereotactic Radiosurgery
Corresponding Author:	Jose Manuel Larraga-Gutierrez Instituto Nacional de Neurologia y Neurocirugia Manuel Velasco Suarez Ciudad de Mexico, CDMX MEXICO
First Author:	Mario Alberto Hernandez Becerril
Order of Authors:	Mario Alberto Hernandez Becerril
	Jose Manuel Larraga-Gutierrez
	Belem Saldivar
	J A Hernandez
Abstract:	The recent publication of the new CoP IEAA/AAPM TRS-483 will allow an accurate measurement of the absorbed dose to water in small and non-standard reference fields in modern radiotherapy. The CoP TRS-483 introduces the use of output correction factors to correct the changes in detector response in relative dosimetry of small photon beams. The output correction factors have generic values for 6 and 10 MV with and without flattening filter regardless of the linear accelerator model except for CyberKnife. The goal of this work was to validate the output correction factor for a 6 MV free flattening filter beam of a TrueBeam STx linac with Monte Carlo simulation for several radiation detectors. The results shown that Monte Carlo calculated output factors and those reported in the CoP TRS-483 agree within 2\% for all the detectors studied in this work. By the later, the use of generic correction factors for a TrueBeam STx is adequate for the dosimetry of small static beams within the uncertainties of Monte Carlo calculations and output correction factors reported in TRS-483.
Suggested Reviewers:	Johnny Morales johnny.morales@lh.org.au Dr. Morales had published several papers on small beam dosimetry using Monte Carlo simulations
	Tracy Underwood tsa.underwood@gmail.com Dr. Underwood had worked in the measurement of output correction factors for small beam dosimetry in the context of TRS-483
Opposed Reviewers:	
Response to Reviewers:	

SALUD
SECRETARÍA DE SALUD

INSTITUTO NACIONAL DE NEUROLOGÍA Y NEUROCIRUGÍA
MANUEL VELASCO SUÁREZ

Dirección de Investigación
Laboratorio de Física Médica

Mexico City, 21st December 2020

Prof. Brian E. Zimmerman
Editor-in-Chief
Applied Radiation and Isotopes Journal

Dear Prof. Zimmerman,

Thanks to you and journal editors for the opportunity to submit the manuscript entitled “Monte Carlo verification of output correction factors for a TrueBeam STx® linac” for review. The effort and the time invested by the reviewers is unvaluable. The authors thank the reviewers’ comments and observations, which helped to improve the quality of our work.

We declare that this manuscript is original, hast not been published before and is not currently being considered for publication elsewhere.

Sincerely,

José Manuel Lárraga Gutiérrez, Ph.D.
Corresponding author
Head Medical Physics Lab
National Institute of Neurology and Neurosurgery
e-mail: jlarraga@innn.edu.mx
Tel. +52 55 56063822 ext. 5021

December 25, 2020

Abstract

Thank you very much to the reviewers and editors Applied Radiation and Isotopes for their work and valuable comments. At what follows, you will find the response to the comments and observations point by point. The modifications to the manuscript were highlighted in color red.

1 Reviewer 2

The article entitled: Monte Carlo Verification of Output Correction factors for a TrueBeam STx deals with verification of correction factors using the TRS-483 Code of Practice for 4 different types of detectors. The novelty lies in the fact that the correction factors were obtained by verification methods. The manuscript has undergone several changes and is now in a more concise format. It is interesting to point out that the in-house model shows superior latency effects when compared to the standard phase space files provided by Varian Medical Systems.

The manuscript can be further improved.
Reviewer's concern (1): Abstract.
Line 38, "By the later", this expression is not used in the English language. Delete this and just start this sentence with "The use of generic correction factors......"

Response: Thanks for your comment. This was fixed as suggested

Reviewer's concern (2): Introduction.
Paragraph two is a bit long and to be honest it is a bit wordy and confusing. In line 25, on page 2, are you referring to the published TRS-483 Code of Practice of the publications by Tanny and Underwood? Can you please clarify this? Perhaps if you start a new paragraph it will become more legible.

Response: Thanks for your comment. Indeed, we refer to the output correction factors published by Tanny and Underwood that which are referenced in TRS-483 as output correction factors determined using the radiation beam of the TrueBeam STx linac.
In response to your comment, we rewrite the second paragraph on page 2 corresponding to the introduction of the article .

Reviewer's concern (3): Paragraph three line 39. "Also, it was developed an in-house Monte Carlo model of the TrueBeam....." change this to "Also, an in-house Monte Carlo model of the Truebeam was developed for the 6 MV FFF photon beam.....”

Response: Thanks for your comment. This was fixed as suggested.

Methods:
Reviewer’s concern (4): Section 2.1.1 line 56. Were these primary electrons or histories?.

Response: Thanks for your comment. Indeed, we refer to the number of primary electrons incident on the x-ray target in the Monte Carlo model of the TrueBeam STx linac that we developed on the BEAMnrc code.

Reviewer’s concern (5): Section 2.1.2 Line 67. Did you run the simulation until the statistical uncertainty achieved was 1% or did you set a fixed number of histories? Please specify.

Response: Thanks for your comment. The simulations were performed using a fixed number of primary histories (3×10^9). With this number of histories a relative statistical uncertainty less than 1% was reached in the Monte Carlo dose profiles.
Reviewer’s concern (6): Section 2.1.4 Line 83. Was the tolerance really 20% ? That is a very high number to be a tolerance, please revise.

Response: Thank you for your comment. The tolerance we use to validate the Monte Carlo depth dose profile in the Buid-up region is correct. This tolerance of 20% is used in the quality assurance for radiotherapy treatment planning systems and is found in Table 4.4 of the reference [19] cited in the work.

Conclusion:
Reviewer’s concern (7): Line 283. You mentioned different linear accelerators and methodologies. But the work presented only dealt with a TrueBeam linac so you cannot really say ”different linear accelerators”.

Response: The sentence was removed to avoid confusion. Also, the adjective ”generic” was added to emphasize that the output correction factors were previously calculated and/or measured using different radiation sources than TrueBeam STx.

2 Reviewer 3

The authors have undertaken a careful revision of the manuscript. I believe it has definitely improved and it is now ready for publication. My feedback has been addressed satisfactorily however I have a few minor comments that should be taken into account before finalising the manuscript. I add them here below:

Reviewer’s concern (1): Page 1, Intro, Line 52: Please replace spread with increased .

Response: Thanks for your comment. This was fixed as suggested .

Reviewer's concern (2): Page 2, Line 41-46: The rationale behind the work is still not clear in this initial part. Are the authors saying that because the values for some chambers have not been measured directly or on a certain machine model they might not be appropriate for a different machine of the same model? Can the authors clarify the sentence "There are outliers possible due to different methodologies, linac properties and beam qualities"? Wouldn't this conclusion apply to any case even when the values were obtained on a specific machine model? .

Response: We agree with your comment. This was fixed as suggested (see lines 11-16 of the new version of the paper).

Reviewer's concern (3): A comment about the novelty of the work has been added in Page 14, line 27-28. The authors could consider highlighting this part in the introduction as well to frame the work.

Response: Thank you very much for your comment. The novelty of the work was highlighted as suggested in the introduction section. The following statement was introduced: "However, in the case of TrueBeam STx® linac, there are no correction factors calculated using Monte Carlo simulation because of vendor restriction on linac's geometry and components' composition."

Reviewer's concern (4): Page 2, Line 49-57: Please revise the structure of this paragraph.
General comment: please replace therefor with "therefore"

Response: Thank you for your comment. This was fixed as suggested.

Reviewer's concern (5): Page 8, Line 56: Please define the reference for the "established tolerances" used to assess the MC model validation.

Response: It was added a reference to sec. 2.1.4 "Monte Carlo tuning and benchmarking". In that section, the tolerances were established to compare Monte Carlo calculated and measured data.

Reviewer's concern (6): Page 11, Line 16: Please replace over respond with over response.
Response: Thank you for your comment. This was fixed as suggested.

Methods:

Reviewer's concern (7): Figure 6 caption, revise front with from.
Response: Thank you for your comment. This was fixed as suggested.

Reviewer's concern (8): Page 13, Line 46: Please replace "it can be notice" with "it can be noticed".

Response: Thank you for your comment. This was fixed as suggested.

3 #Receiving editor comments:

Please address also the following revisions. - Remove the numbering of the lines. The lines are numbered automatically in the submission. Then:

1. In the abstract (submitted as a independent field): typo in flatting. It should be “flattening”.

   Response: Thank you for your comment. The typo was fixed as suggested.

2. “The work of Alfonso et al. have been adopted” → “The work of Alfonso et al. has been adopted”.
   Response: Thank you for your comment. This was fixed as suggested.

3. Line 32, page 2: “at a nominal energies” → “at nominal energies”
   Response: Thank you for your comment. This was fixed as suggested

4. Typo at line 43 of page 2: “dectors’ output”
   Response: Thank you for your comment. This was fixed as suggested.

5. Line 43 at page 2: “Therefor,” →” Therefore,”
   Response: Thank you for your comment. This was fixed as suggested.

6. “The manufacturer provided us with details linac components” → “The manufacturer provided details linac components...” it is clear that the manufacturer gave you the details.
   Response: Thank you for your comment. This was fixed as suggested.

7. “so that the MC dose calculation match experimental measurements” → “so that the MC dose calculation matches the experimental measurements”
   Response: Thank you for your comment. This was fixed as suggested.

8. Line 58 page 4: “The above process also was followed” → “The above process was also followed...”
   Response: Thank you for your comment. This was fixed as suggested

9. Line 59, page 4: “OAR profile from a 10 cm x10 cm field size” → “OAR profile obtained with a 10 cm x10 cm field size”
   Response: Thank you for your comment. This was fixed as suggested

10. Beginning of page 5: “once the MC model of ... was validated, PHPS ....”
    Response: Thank you for your comment. This was fixed as suggested.

11. Line 39, page 5: “denote the absorbed dose to the detector’s sensitive volume and Qfmsr and Qfclin stands for the radiation beam quality of the field sizes fmsr and fclin.” → “denote the absorbed dose to the detector’s sensitive volume. Qfmsr and Qfclin stand for the radiation beam quality

of the field sizes fmsr and fclin, respectively."
Response: Thank you for your comment. This was fixed as suggested.

12. "The terms associated with equation (1) are calculated by using MC simulation of radiation transport." →"The terms associated with equation (1) are calculated by means of MC simulations."
Response: Thank you for your comment. This was fixed as suggested.

13. "egs_chamber" should always be in Courier, while sometimes it is in Times New Roman. Please check thoroughly the text.
Response: Thank you for your comment. This was fixed as suggested.

14. Line 36 page 6: "by linac's manufacturer" → "by the linac's manufacturer"
Response: Thank you for your comment. This was fixed as suggested.

15. line 46 page 6: "tow fold." → I think the authors mean" two fold".
Response: Thank you for your comment. This was fixed as suggested.

16. Fig 4 and 5: state in the caption the accuracy of the experimental measurements. It seems to me this information is missing in the paper.
Response: The following statement was added to each figure caption: The uncertainty of the measured data was less than 0.3% on average (min. 0.1%, max. 0.5%).

Highlights

- The $k_{Qclin,Qmsr}^{fclin,fmsr}$ of 4 radiation detectors were calculated for a TrueBeam STx
- The calculated $k_{Qclin,Qmsr}^{fclin,fmsr}$ were compared to those reported in IAEA/AAPM TRS-483
- An agreement within 1% was found between calculated and reported $k_{Qclin,Qmsr}^{fclin,fmsr}$
- The reported values in TRS-483 are reliable for a TrueBeam STx linac

Declaration of interests

☒ The authors declare that they have no known competing financial interests or personal relationships that could have appeared to influence the work reported in this paper.

☐The authors declare the following financial interests/personal relationships which may be considered as potential competing interests:

INSTITUTO NACIONAL DE NEUROLOGÍA Y
NEUROCIRUGÍA MANUEL VELASCO SUÁREZ

Mexico City, April 3rd 2020

Mario A. Hernández-Becerril: Methodology, Software, Writing-Original Draft, Investigation

José M. Lárraga-Gutiérrez: Conceptualization, Methodology, Validation, Writing-Review & Editing, Supervision

Belem Saldívar: Data Curation, Writing-Review & Editing

J.A. Hernández-Servín: Data Curation, Visualization

Monte Carlo Verification of Output Correction Factors for a TrueBeam STx®

Mario A. Hernández-Becerril[a], José M. Lárraga-Gutiérrez[b], Belem Saldivar[a,c], J.A. Hernández-Servín[a]

[a]*Facultad de Ingeniería, Universidad Autónoma del Estado de México, Cerro de Coatepec s/n, Ciudad Universitaria, Toluca 50100, Estado de México, México*

[b]*Laboratorio de Física Médica, Instituto Nacional de Neurología y Neurocirugía, Insurgentes sur 3877, Tlalpan 14269, CDMX, México*

[c]*Cátedras CONACYT, Av. Insurgentes sur 1582, Col. Crédito Constructor, Alcaldía Benito Juárez, CDMX 03940, México*

Abstract

The recent publication of the new code of practice IEAA/AAPM TRS-483 introduces the use of output correction factors to correct the changes in detector response in relative dosimetry of small photon beams. In TRS-483, average correction factors are reported for several detectors at 6 and 10 MV with and without flattening. These correction factors were determined by Monte Carlo simulation or experimental measurements using several linacs of different brands and vendors. The goal of this work was to validate the output correction factors reported in TRS-483 for a 6 MV (with and without flattening filter) of a TrueBeam STx® linac with Monte Carlo simulation for four radiation detectors employed in the dosimetry of small photon beams and whose output correction factors were determined using different radiation source than TrueBeam STx®: PTW®31010, PTW®31016, IBA®CC-01, and IBA®SFD. The results show that Monte Carlo calculated output factors, and those reported in the code of practice TRS-483 fully agree within ∼1%. The use of generic correction factors for a TrueBeam STx® and the detectors studied in this work is adequate for small dosimetry static beams within the uncertainties of Monte Carlo calculations and output correction factors reported in TRS-483.

Key words: TRS-483, Monte Carlo simulation, output correction factors, detector model, Phase Space File, Latent Variance.

---

1. Introduction

The development of new treatment modalities in radiotherapy, such as intensity-modulated radiation therapy and stereotactic radiosurgery, has increased the use of small photon fields [1, 2]. By following a well-established Code of Practice (CoP) for reference dosimetry in standard fields (such as IAEA TRS-398 [3]), measurement of absorbed dose to water in small radiation fields requires additional corrections to those established in TRS-398 because the detector's response is influenced by different physical factors related to the small field and the detector itself. The main physical factors are radiation

*Corresponding author
Email address: jlarraga@innn.edu.mx (José M. Lárraga-Gutiérrez)

source occlusion, loss of lateral electronic equilibrium, and the detector's average volume effect [4]. Alfonso et al. [5] proposed a formalism that relates the reference dosimetry in conventional fields to that in small static fields by means of an output correction factor ($k^{f_{clin},f_{msr}}_{Q_{clin},Q_{msr}}$) that corrects for the changes in detector response between the machine-specific reference field (f_{msr}) and the small clinical field (f_{clin}). The $k^{f_{clin},f_{msr}}_{Q_{clin},Q_{msr}}$ depends on the radiation detector and can be determined experimentally or by Monte Carlo (MC) simulation.

The work of Alfonso et al. has been adopted in the technical report TRS-483 published by the International Atomic and Nuclear Energy Agency (IAEA) and the American Association of Physicists in Medicine (AAPM) [6]. This report provides generic correction factors calculated by averaging the output correction factors reported by several research groups for many radiation sources and detectors employed in small field dosimetry [6]. Overall, the $k^{f_{clin},f_{msr}}_{Q_{clin},Q_{msr}}$ values were calculated through MC simulation or determined experimentally [7–13].

The reported $k^{f_{clin},f_{msr}}_{Q_{clin},Q_{msr}}$ in TRS-483 are intended to be independent ~~of~~ radiation source vendor. The correction factor's value depends on the specif detector of interest and the radiation field size at nominal energies of 6 MV and 10 MV. However, in the case of TrueBeam STx® linac, there are no correction factors calculated using Monte Carlo ~~simulation~~ because of vendor restriction on linac's geometry and components' composition. The $k^{f_{clin},f_{msr}}_{Q_{clin},Q_{msr}}$ values reported in the TRS-483, where the TrueBeam STx® linac was used as a radiation source, were measured by two research groups [14, 15] using the detectors Sun Nuclear EDGE™, Exradin® A14SL, A16, A26 and PTW®31014, 60017, 60019. Therefore, it would be important to verify if the detectors' output correction factors are applicable for a TrueBeam STx® machine when they are calculated or measured using a different linac.

The goal of this work is to show that the reported $k^{f_{clin},f_{msr}}_{Q_{clin},Q_{msr}}$ in TRS-483 for 4 radiation detectors are adequate to be used in photon beams of 6 MV (WFF and FFF) of a TrueBeam STx® linac within the uncertainties established by the CoP TRS-483. In order to do so, $k^{f_{clin},f_{msr}}_{Q_{clin},Q_{msr}}$ values were calculated by MC simulation for PTW® 31010, 31016 and IBA® CC01 and SFD radiation detectors, and compared to those reported in the CoP TRS-483. Also, an in-house MC model of the TrueBeam STx® linac was developed for 6 MV FFF photon beams based on the work of Rodriguez et al. [16].

2. Materials and Methods

2.1. MC model of Varian TrueBeam STx® linac

2.1.1. MC linac head model

A model of a TrueBeam STx® linac was developed based on a linac Clinac 2100 ® (Varian Medical Systems, Palo Alto, California, USA) for Monte Carlo simulation. The manufacturer provided details of the linac components, geometry, and materials under a non-disclosure agreement. According to Rodríguez et al. [16], it is possible to simulate a 6 MV FFF beam of a TrueBeam STx® by modifying some components of the Clinac 2100®. The proposed TrueBeam STx® model considered the geometry and materials of X-ray target, collimators (primary and secondary), and a modified version of the flattening filter (FF). The modified version of the FF eliminates electron contamination arising from the target and allows it to simulate free flattening filter (FFF) photon beams (see Figure 1). The parameters associated with the primary electron beam such as electron beam energy (E), the standard deviation of the Gaussian radial distribution ($\sigma_x = \sigma_y = \sigma$) and beam's divergence (φ) were adjusted so that the MC dose calculation matches the experimental measurements (see 2.1.4). Parameter values were within the interval of 5.8-6.2 MeV, 0-0.15 cm and 0-0.1° for E, σ and ϕ, respectively. Additional parameters in `BEAMnrc` for the linac head simulation were $5{\times}10^8$ primary electrons incident on the x-ray target, the cutting energy for electrons (ECUT), and photons (PCUT) were set to 0.7 and 0.01 MeV, respectively. Directional Bremsstrahlung splitting with a 1000 and radius value depending on the simulated field size and ESAV 0.1 MeV.

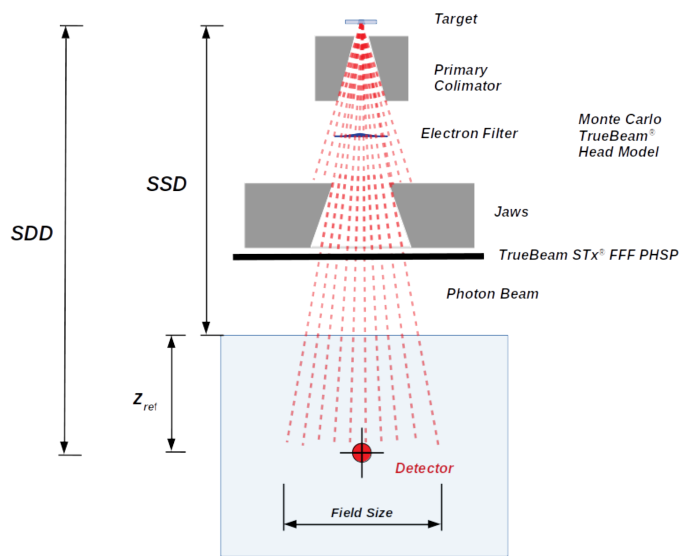

Figure 1: Geometric conditions for the calculation of output correction factors $k^{f_{clin},f_{msr}}_{Q_{clin},Q_{msr}}$ using `egs_chamber` user code. The figure shows a diagram of the considered components for the TrueBeam STx® linac model. The electron filter stands for the modified flattening filter used to remove electron contamination.

2.1.2. Dose profile calculation

The `DOSXYZnrc` code was used to calculate the percentage depth dose (PDD) and off-axis (Cross-Plane) dose profiles (OARs) at a depth of 10 cm, with SSD=100 cm. Dose profiles calculation (PDD and OARs) was performed by simulating a cube phantom made of water with dimensions of 30 cm×30 cm×30 cm segmented in voxels of $0.25 \times 0.25 \times 0.25$ cm^3 (in the z direction for the PDD, and x direction for the OARs). The additional parameters in `DOSXYZnrc` were ECUT = 0.911 MeV, PCUT = 0.01 MeV, $N_{recycl} = 15$, HOWFARLESS turned on and the photon splitting option with a value of 50. To obtain a relative statistical uncertainty equal or less than 1% in the calculated dose profiles, the number of primary histories employed ~~on~~ the MC simulation ~~were~~ 3×10^9.

2.1.3. Dose profile measurements

The experimental measurements for depth dose (PDDs) and off-axis profiles (OARs) were performed under the same conditions as MC calculations. Measurements were carried out using a mini-ionization chamber PTW-31016 (PTW-Freiburg, Germany) and a beam scanning system (MP3-M, PTW-Freiburg, Germany) with its associated software (Mephysto MC^2, PTW-Freiburg, Germany). The ionization chamber was utilized for field sizes ≥ 3 cm length size, while for small fields (< 3 cm), ~~it was employed~~ a microDiamond detector (PTW-60019, PTW-Freiburg, Germany)

2.1.4. MC tuning and benchmarking of the linac model

In this work, the `BEAMnrc` parameter optimization was performed by following the work of Almberg et al. and Wang et al. [17, 18]. Overall, the fine-tuning procedure consists of minimizing the local dose differences ($\Delta(\%)$) between calculated and measured dose profiles (depth and off-axis) for a 5 cm$\times$5 cm field size. The electron beam's energy (E) was tuned using PDD, while the beam intensity width (σ) and beam divergence (φ) were tuned using OARs. For E, the energy value was changed from 5.8 to 6.2 MeV in 0.1 MeV steps. The optimal value of E was the one that minimizes the slope of the linear function of $\Delta(\%)$ vs depth (z). Likewise, the average local dose difference in ($z < d_{max}$) and outside ($z > d_{max}$) the build-up region was calculated. It was established a tolerance of ~~20%~~ and 2% [19] for in and outside the build-up region, respectively. It is also expected that the calculated $TPR_{20,10}$ match the experimental beam quality $TPR_{20,10} = 0.629$.

For the electron beam's radial intensity width (σ), the adjustment was carried out by analyzing the differences between MC calculated and measured dose off-axis profiles. Local differences ($\Delta(\%)$) were evaluated between calculated and measured OAR profiles for the central dose region (100-80% of the dose). The tolerance was established for the central region to be $< 2\%$. The penumbra region (80-20% dose) was analyzed by evaluating the local differences at points within ± 2.0 mm from the 50% dose region (field edge)[17]. The local differences were root mean squared (RMS); the σ with minimum RMS would describe the best match between MC calculation and profile measurements. The above process was also followed to adjust the angular divergence of the beam (φ). The angular divergence optimization was performed using an OAR profile obtained with a 10 cm$\times$10 cm field size [17]. Once the MC model of the TrueBeam STx® linac was validated, PHSP files were calculated for the following field sizes shaped by the jaw collimators: 0.5×0.5, 1×1, 1.5×1.5, 2×2, 3×3, 4×4, 6×6 and 10×10 cm^2.

2.2. Calculation of $k^{f_{clin},f_{msr}}_{Q_{clin},Q_{msr}}$ in static fields

According to the formalism proposed in TRS-483 for static fields, the output correction factor for a specific detector is defined as

Property	PTW-31010	PTW-31016	IBA-CC01	IBA-SFD
Type	IC	IC	IC	Solid State
Sensitive volume	Air 0.125 cm^3 Ø 5.5 mm, length=6.5 mm	Air 0.016cm^3 Ø 1.90 mm, length=2.9 mm	Air 0.01 cm^3 Ø 2.0 mm, length=3.6 mm	Silicon 0.170×10^{-3} cm^3 Ø 0.6 mm, length=0.06 mm
Wall thickness	0.7 mm 0.57 mm PMMA ($\rho = 1.19\,\mathrm{g/cm^3}$) 0.13 mm graphite ($\rho = 0.82\,\mathrm{g/cm^3}$)	0.66 mm 0.57 mm PMMA ($\rho = 1.19\,\mathrm{g/cm^3}$) 0.09 mm graphite ($\rho = 0.82\,\mathrm{g/cm^3}$)	0.50 mm 0.5 mm C_{552} ($\rho = 1.76\,\mathrm{g/cm^3}$)	Not apply
Electrode	Al, graphite coated Ø 1 mm, length=5 mm	Al Ø 0.3 mm, length=1.6 mm	Steel Ø 0.35 mm, length=2.6 mm	Not apply

Table 1: Main characteristics of the detector modeled in this work for MC simulations. The information was collected from the blueprints. The letters ”IC” stand for ionization chamber.

$$k^{f_{clin},f_{msr}}_{Q_{clin},Q_{msr}} = \frac{D^{f_{clin}}_{w,Q_{clin}}/\bar{D}^{f_{clin}}_{det,Q_{clin}}}{D^{f_{msr}}_{w,Q_{msr}}/\bar{D}^{f_{msr}}_{det,Q_{msr}}} \tag{1}$$

where $D^{f_{clin}}_{w,Q_{clin}}$ and $D^{f_{msr}}_{w,Q_{msr}}$ denote the absorbed dose in water in the absence of the detector for the clinical small field (f_{clin}) and the machine specific reference field (f_{msr}). $\bar{D}^{f_{msr}}_{det,Q_{msr}}$ and $\bar{D}^{f_{clin}}_{det,Q_{clin}}$ denote the absorbed dose to the detector's sensitive volume. Q_{fmsr} and Q_{fclin} stand for the radiation beam quality of the field sizes f_{msr} and f_{clin}, respectively.

The terms associated with equation (1) are calculated by means of MC simulations. The MC simulation requires the complete model of the detector to calculate the terms $\bar{D}^{f_{msr}}_{det,Q_{msr}}$ and $\bar{D}^{f_{clin}}_{det,Q_{clin}}$ in its active volume, as well a point-like water volume to calculate $D^{f_{clin}}_{w,Q_{clin}}$ and $D^{f_{msr}}_{w,Q_{msr}}$. Following the methodology described above, $k^{f_{clin},f_{msr}}_{Q_{clin},Q_{msr}}$ and its expanded uncertainty (uncertainty type A [20]) were calculated by modeling using `egs_chamber` the detectors PTW-31010 (PTW-Freiburg, Germany), PTW-31016 (PTW-Freiburg, Germany), IBA-CC01 (IBA-Dosimetry, Germany), IBA-SFD (IBA-Dosimetry, Germany) and small water volume (voxel) of $0.05 \times 0.05 \times 0.05$ cm^3. $D^{f_{clin}}_{w,Q_{clin}}$ and $D^{f_{msr}}_{w,Q_{msr}}$ were calculated by replacing each detector model with a water voxel located at the effective point of measurement of the detector (see Figure 2). Detectors main characteristics are shown Table 1. The calculation geometry setup was SSD=90 cm with a $z_{ref} = 10$ cm. Dose calculation on detectors and water voxel was performed inside a water phantom of 30 cm×30 cm×cm size.

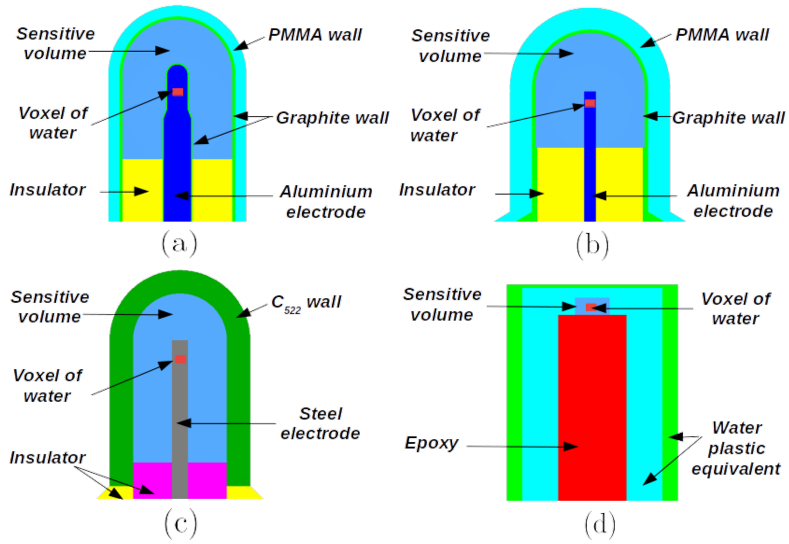

Figure 2: Schematic diagram of detectors' components modeled using `egs_chamber` for (a) PTW-31010, (b) PTW-31016, (c) IBA -CC01 and (d) IBA-SFD radiation detectors. The water voxel shows the position of the detector's effective point of measurement. The effective point of measurement and the water voxel's center was positioned at 10 cm depth in their respective simulations.

Two different approaches were performed to calculate $k_{Q_{clin},Q_{msr}}^{f_{clin},f_{msr}}$. The first approach consisted of using an in-house developed model of the TrueBeam STx® linac as described in section (2.1.1) for particle source simulation. The MC linac model only simulates 6 MV photon beams free of flattening filter (FFF). The second approach consisted of using the Varian phase-space files provided by the linac's manufacturer for particle source simulation. The linac manufacturer provides 50 phase-space files for 6 ~~MV flattened (WFF) and unflattened (FFF)~~ photon beams each of a TrueBeam STx® linac. All the phase space files are recorded close and behind the upper jaws. The 50 phase-space files were added to get a single phase-space file (Varian Primary FFF/WFF PHSP, see Figure 3) for each filter modality. A simple simulation was configured only to include the secondary jaws to shape the beam. The calculated output correction factors using both approaches were compared to those reported in TRS-483. The purpose of this comparison was two fold. The first was to evaluate the behavior of the $k_{Q_{clin},Q_{msr}}^{f_{clin},f_{msr}}$ calculated with photon beams obtained with two different MC models for the same linac for 6 MV FFF beams. The second was to observe any significant difference between calculated $k_{Q_{clin},Q_{msr}}^{f_{clin},f_{msr}}$ for flattened and unflattened beams. For simplicity and ~~for~~ reduce computational costs, only the output correction factors ($k_{Q_{clin},Q_{msr}}^{f_{clin},f_{msr}}$) of detector IBA-CC01 were calculated using the two approaches described above for flattened and unflattened beams.

In all detector simulations, photon cross-section enhancement (XCSE) was used with an enhancement factor of 128 in a cylindrical water volume around each detector model's sensitive volume. The XCSE is a variance reduction technique (VRT) that improves the efficiency of the MC simulation

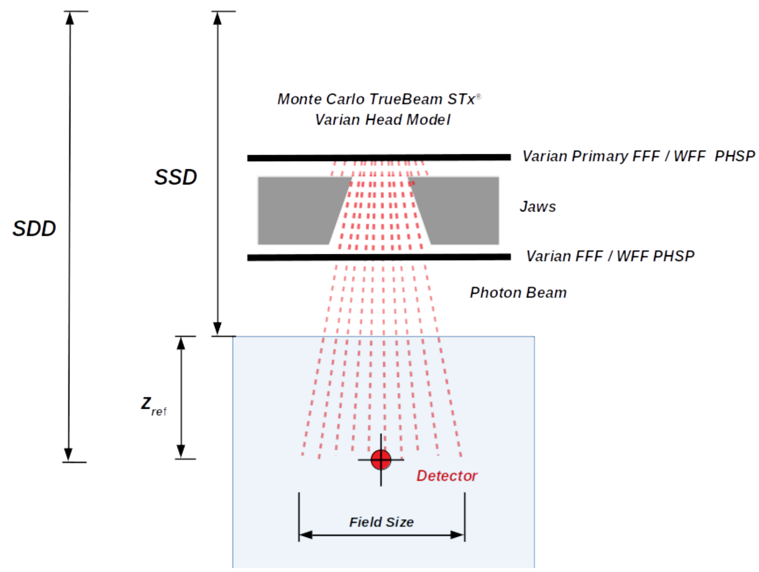

Figure 3: Geometric conditions for the calculation of output correction factors $k^{f_{clin},f_{msr}}_{Q_{clin},Q_{msr}}$ using the Varian FFF and FFF PHSP in the `egs_chamber` user code. The figure shows the position of the Varian Primary, FFF and WFF PHSP used in the simulations.

utilizing an enhancement factor. The enhancement factor weights the photon cross-section, which decreases the mean free path and increases the production of charged particles along the path of each simulated photon [21]. The additional parameters in the `egs_chamber` code were ECUT=0.07 MeV, PCUT=0.01 MeV and N_{recycl}=20. The number of histories in MC simulations were chosen in a way that the expanded uncertainty on the detector response in the f_{clin} ($D^{f_{clin}}_{w,Q_{clin}}/\bar{D}^{f_{clin}}_{det,Q_{clin}}$) and f_{msr} ($D^{f_{msr}}_{w,Q_{msr}}/\bar{D}^{f_{msr}}_{det,Q_{msr}}$) field was less than 0.5% and consequently the total uncertainty in the $k^{f_{clin},f_{msr}}_{Q_{clin},Q_{msr}}$ values were less than 1%.

2.3. Evaluation of the latent variance of MC linac model

The statistical uncertainty of the absorbed dose calculated by MC simulation depends on the number of histories used and can be reduced to a limit from which it no longer changes. This statistical uncertainty limit is known as *latent variance* (LV) [22]. The work of Alhakeem et al. [23] was followed to evaluate the LV of the PHSP files generated by the MC linac model. The dose and its variance (in percentage) were calculated using `DOSXYZnrc` user code. The dose was calculated in voxels of $0.01 \times 0.01 \times 0.01$ cm^3 and $0.3 \times 0.3 \times 0.3$ cm^3. The voxels were placed at the central beam axis at a depth of 10 cm inside a water phantom of $30 \times 30 \times 30$ cm^3. The water voxel size was chosen to be equivalent to that of the detector's sensitive volume. MC simulations were performed for each field size for N_{recycl} parameter equal to 50, 100, 200, 300, 400, and 500. For each simulation, the dose variance was recorded. The dose variance shows a linear behavior as a function of $1/N_{recycl}$ [17]. Then, the LV was determined by extrapolating the dose variance for $1/N_{recycl}$ equal to zero (N_{recycl} approaches to infinity).

3. Results and Discussion

3.1. MC linac model: tuning and benchmarking

Figure 4a shows a comparison between the calculated and measured depth dose curves for a 5 cm$\times$ 5 cm field size. Good agreement can be observed between calculated and measured depth dose curves for electron beam energies between 5.8 and 6.2 MeV. Local differences ranged from 2.4 to 3.5% and 0.8 to 2.6% for inside and outside build-up regions. Nevertheless, the PDD calculated with an electron beam energy of 5.8 MeV showed a better match with experimental data. For 5.8 MeV, local differences showed the minimum values for inside ($< 2.4\%$) and outside ($< 0.8\%$) the build-up region. For this beam energy, the slope $m_\Delta = -0.056$ was closest to zero (see Figure 4b) from the calculated PDD curves. A PDD was calculated using a $E = 5.8$ MeV for the machine reference field size of 10×10 cm^2. The calculated $\mathrm{TPR}_{20,10}$ for the reference field was 0.626. A comparison between the MC calculated and experimental $\mathrm{TPR}_{20,10} = 0.629$ showed an absolute difference of $<$ 0.5%.

Figure 4c shows the Monte Carlo and measured OARs for σ values between 0.0 and 0.1 cm. As can be seen, all the calculated profiles showed an acceptable agreement with measured profiles in the central region within the established tolerances ($< 2\%$). For the central region, local differences ranged from 0.15 to 0.30%. For the penumbra region, RMS values ranged from 0.9 to 4.6%. The profile with $\sigma = 0.05$ cm showed the lowest average local differences for the central ($< 0.3\%$) and penumbra regions ($RMS = 0.9\%$) between calculated and measured data (see Figure 4d). The $\sigma = 0.05$ cm is equivalent to a full width at half-maximum (FHWM) of 1.2 mm; this value is consistent with those reported by other authors for the TrueBeam STx® linac [24, 25], which reported focal spot sizes between 1.1 to 2.5 mm for this linac.

Figure 5(a) shows a comparison between MC calculated and measured 10 $\times$ 10 cm field size profile. Fixing $E = 5.8$ MeV and $\sigma = 0.05$ cm, the electron beam angle divergence was tuned to $\varphi = 0.02°$. The local differences were 0.4 and 2.2% for the central and penumbra regions (RMS), respectively. The above results showed that the optimal values to simulate the TrueBeam STx® linac were $E = 5.8$ MV, $\sigma = 0.05$ cm and $\varphi = 0.02°$. Off-axis dose profiles for small fields were calculated using these optimized parameters. Figure 5b shows a comparison between MC simulation and measured profiles for square small fields of 0.5, 1.0 and 2.0 cm length size. Good agreement can be observed between calculations and measurements. Average local differences for the central region were less than 0.5%, and for the penumbra region, less than 3.8% for 1.0 and 2.0 cm field sizes. For the smallest field size, local differences were 1.4% and 4.1% for central and penumbra (RMS) regions, respectively. All the observed differences were within the established tolerances (see Sec. 2.1.4). Overall, the MC linac model showed a good agreement with experimental data for conventional and small fields.

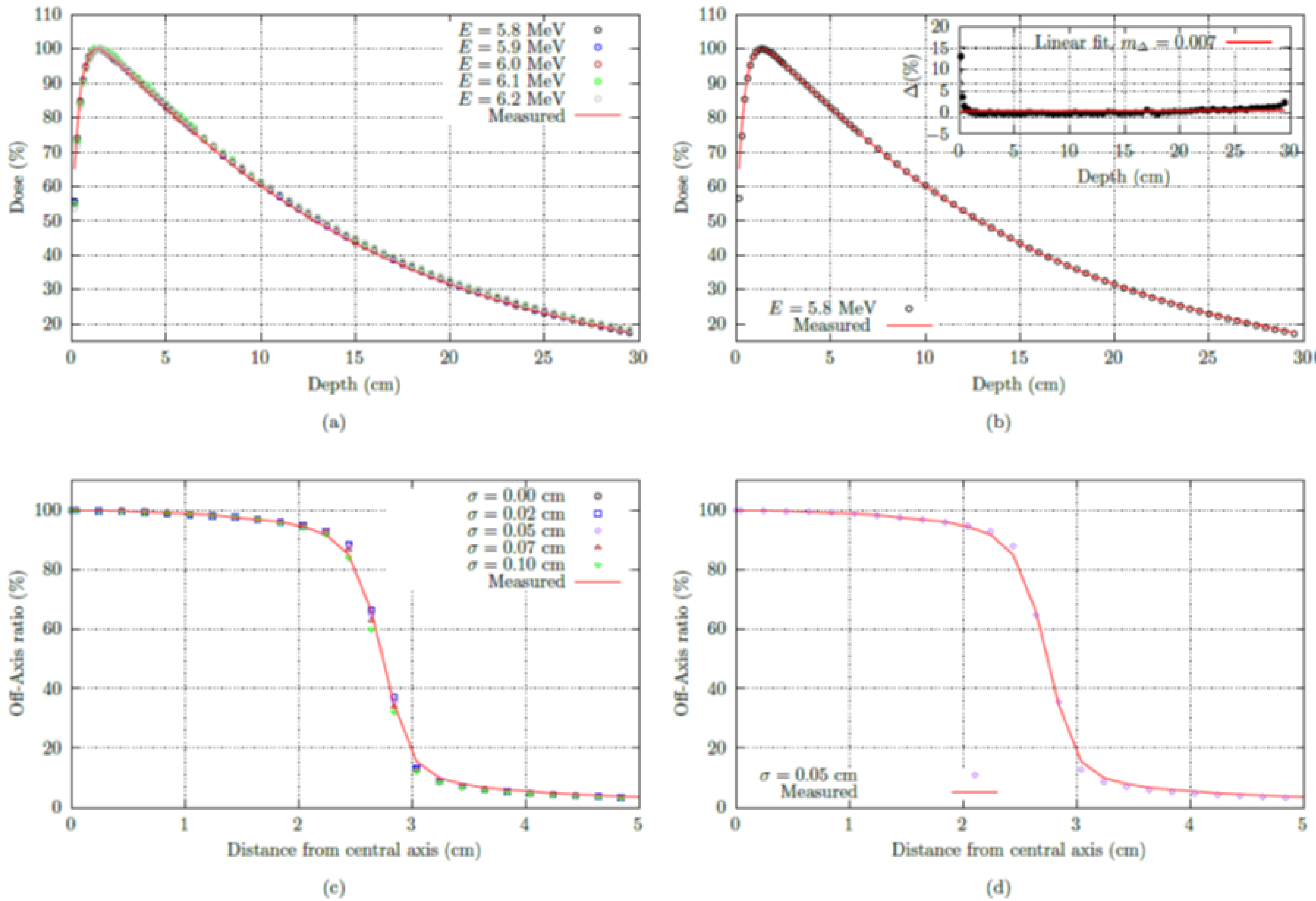

Figure 4: Graphical comparison of the dose profiles measured and calculated with MC simulation for a field size of 5×5 cm^2. (a) Calculated depth dose profiles (PDD) for different electron beam energies ($\sigma = 0.00$ cm, $\varphi = 0°$), (b) calculated depth dose profile for an electron's energy of 5.8 MeV. The inset shows the linear fit of local differences ($\Delta\,(\%)$) as a function of depth in water. (c) Calculated OARs for different values of σ ($E = 5.8$ MeV, $\varphi = 0°$) for a field size of 5 cm $\times$ 5 cm, and (d) calculated OAR for $\sigma = 0.05$ cm (FWHM = 1.2 mm). The relative statistical uncertainty associated with the dose profiles calculated with MC simulation is less than 0.5%. The uncertainty of the measured data was less than 0.3% on average (min. 0.1%, max. 0.5%).

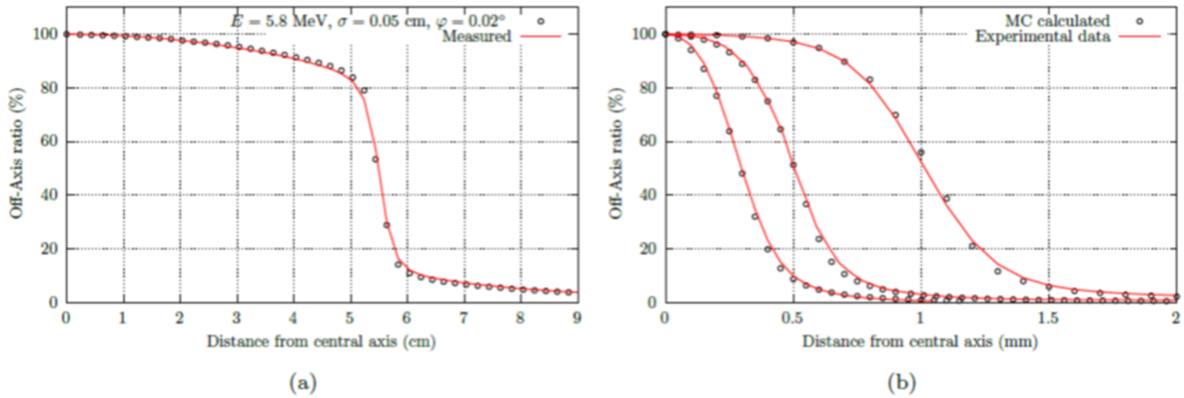

Figure 5: Graphical comparison between measured and MC calculated off-axis profiles for a field size of 10 cm×10 cm (a) and small fields (b). It is shown in increasing width order 0.5, 1.0, and 2.0 cm field sizes. The relative statistical uncertainty associated with the calculated OAR is less than 0.5%. The uncertainty of the measured data was less than 0.3% on average (min. 0.1%, max. 0.5%).

	$k^{f_{clin},f_{msr}}_{Q_{clin},Q_{msr}}$			
f_{clin} (cm^2)	PTW-31010	PTW-31016	IBA-CC01	IBA-SFD
6×6	$1.003 \pm 0.598\%$	$1.006 \pm 0.545\%$	$1.004 \pm 0.559\%$	$1.018 \pm 0.493\%$
4×4	$1.000 \pm 0.509\%$	$1.002 \pm 0.543\%$	$1.007 \pm 0.557\%$	$1.020 \pm 0.438\%$
3×3	$1.001 \pm 0.594\%$	$1.005 \pm 0.455\%$	$1.009 \pm 0.463\%$	$1.021 \pm 0.351\%$
2×2	$1.002 \pm 0.499\%$	$1.002 \pm 0.639\%$	$1.007 \pm 0.465\%$	$1.024 \pm 0.350\%$
1.5×1.5	$1.017 \pm 0.491\%$	$1.014 \pm 0.539\%$	$1.013 \pm 0.462\%$	$1.029 \pm 0.345\%$
1×1	–	$1.028 \pm 0.443\%$	$1.013 \pm 0.461\%$	$1.016 \pm 0.528\%$
0.5×0.5	–	–	–	$0.986 \pm 0.554\%$

Table 2: MC calculated correction factors ($k^{f_{clin},f_{msr}}_{Q_{clin},Q_{msr}}$) and their expanded uncertainty (%) as a function ~~on~~ the field size (f_{clin}) in the `egs_chamber` code. The expanded uncertainty has a coverage factor $k = 1$. The PHSP obtained with the MC model of the Varian TrueBeam STx® linac developed on `BEAMnrc` was used as the particle source for the simulations.

3.2. Calculation of $k^{f_{clin},f_{msr}}_{Q_{clin},Q_{msr}}$ in static fields

Table 2 shows the MC output correction factors and their statistical uncertainty calculated using MC linac model with `egs_chamber` user code. As can be observed, for the ionization chambers and for field sizes ≤ 2.0 cm, the $k^{f_{clin},f_{msr}}_{Q_{clin},Q_{msr}}$ were close to unity (within 1.0%). For field sizes > 2.0 cm, the $k^{f_{clin},f_{msr}}_{Q_{clin},Q_{msr}}$ were within 1.5 and 3% from unity. The behavior of the ionization chambers is due to three effects: (i) the average volume effect due to the dimensions of the active volume of the detector relative to the field size, which causes the sensitive volume to not be irradiated with a uniform energy fluence [4], (ii) the lateral electron equilibrium (LEE), which occurs when the size of the f_{clin} is smaller than the range that electrons have in water r~~ealtiv~~e to the active volume material which makes the dose-collisional kerma ratio (D/K_c) be less than 1 [26], and (iii) the density of the active volume, since if it is less than the water density, the absorbed dose at a point of interest in the active volume of the detector will be low compared to that registered by the water at that point, which leads to its sub-response.

For the IBA-SFD silicon detector, the $k_{Q_{clin},Q_{msr}}^{f_{clin},f_{msr}}$ are greater than the unity up to $\sim 3\%$ for field sizes greater than 0.5×0.5 cm^2. In the f_{clin} interval of 1.5×1.5 to 6×6 cm^2 the correction factor increases as the field size decreases. For $f_{clin} < 1.5 \times 1.5$ cm^2 the correction factor decreases, indicating that in this field the detector over-response begins to increase. This behavior is due to the difference in the photoelectric cross sections at low energies of silicon compared to water, causing the silicon to be more sensitive to low energy photons [11] at the reference field. The loss of electronic lateral equilibrium and the active volume density impact the detector's response for the IBA-SFD model at the smallest field sizes, increasing the trend to over-response [27]. Figure 6 shows a comparison between $k_{Q_{clin},Q_{msr}}^{f_{clin},f_{msr}}$ calculated for each detector in this work and those reported in TRS-483. Good agreement can be observed for all the MC modeled detectors. The differences between the output correction factors are within the uncertainty band. For the detector IBA-CC01 (Figure 6c), the calculated correction factors not only showed an excellent agreement compared to those reported in the CoP. Moreover, it can be observed that the differences are the smallest of all the ionization chambers modeled in this study. The latter may be attributed to the fact that the IBA-CC01 ionization chamber has a unique wall made of air-equivalent plastic material, simplifying the geometry and difficulty of the radiation transport on the MC simulation.

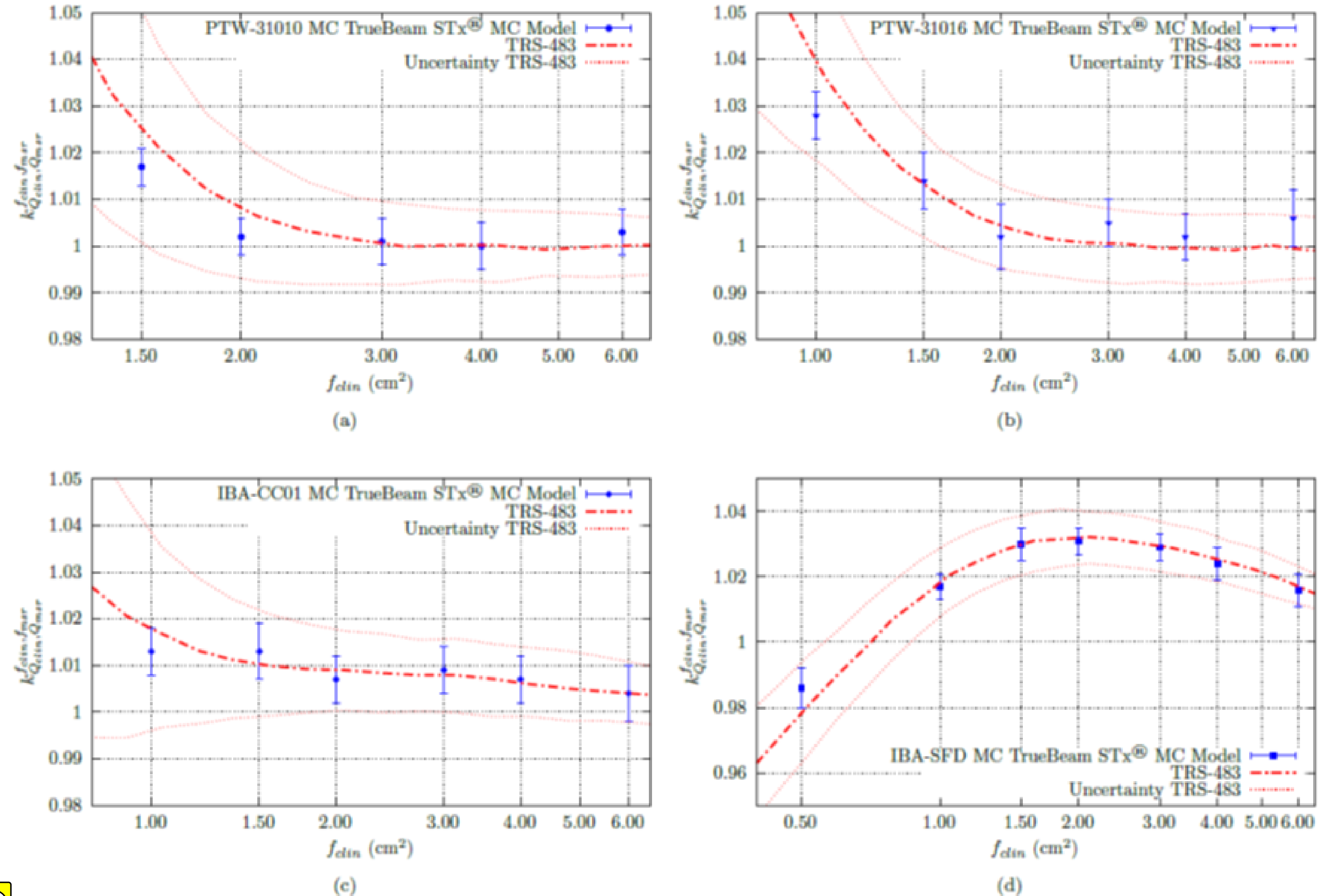

Figure 6: Graphical comparison of the output correction factors ($k^{f_{clin},f_{msr}}_{Q_{clin},Q_{msr}}$) calculated in this work with those reported in the TRS-483 for each detector model (in logarithmic scale): (a) PTW-31010, (b) PTW-31016, (C) IBA-CC01, (d) IBA-SFD. The dashed thick lines represent the values reported by TRS-483. The dotted lines represent the correction factors' uncertainty, as reported in TRS-483 (see Table 26 and 37 from the CoP TRS-483).

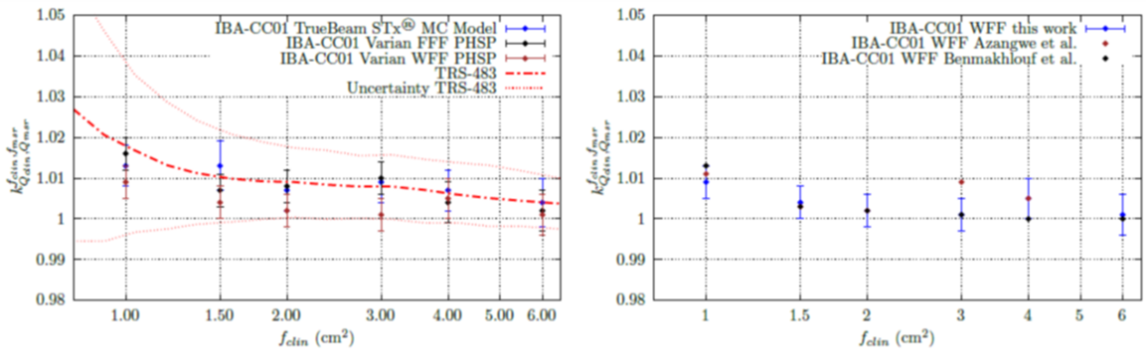

(a) (b)

Figure 7: (a) Graphical comparison of the MC correction factors ($k^{f_{clin},f_{msr}}_{Q_{clin},Q_{msr}}$) for the IBA-CC01 mini-ionization chamber. The $k^{f_{clin},f_{msr}}_{Q_{clin},Q_{msr}}$ were calculated using the MC model of the TrueBeam STx® and the Varian PHSP files for 6 MV WFF and FFF beams. The dashed thick line represents the values reported by TRS-483. The dotted lines represent the uncertainty associated with the average values reported in TRS-483. (b) Comparison of output correction factors calculated in this work and those calculated by Azangwe et al.[28] and Benmakhlouf et al.[29] for 6 MV WFF beams. The data from Azangwe et al. was determined experimentally while the data of Benmakhlouf et al. was calculated using PENELOPE.

3.3. Comparison of output correction factors for the IBA-CC01 detector using different sources

Figure 7a shows $k^{f_{clin},f_{msr}}_{Q_{clin},Qmsr}$ for the IBA-CC01 ionization chamber using different radiation sources. Good agreement can be observed for all the calculated correction factors compared to those of TRS-483 for this mini-ionization chamber. All the differences did not exceed 1%, and were within the uncertainty band for all the field sizes. There were no significant differences between the calculated $k^{f_{clin},f_{msr}}_{Q_{clin},Qmsr}$ using Varian PHSP files and our linac model within the uncertainties for 6 MV FFF beams. Nevertheless, as can be seen in section 3.4, our linac model's advantage was to have an LV lower than the LV of Varian PHSP files. Also, the differences were not significant between output correction factors calculated for flattened and unflattened beams. This result reinforces using a single correction factor for unflattened and flattened photon beams, as stated by TRS-483. However, it can be noticed that $k^{f_{clin},f_{msr}}_{Q_{clin},Qmsr}$ for 6 MV WFF beams had a trend to be below the average values from TRS-483. The opposite happened for unflattened beams. The observed differences between output correction factors for flattened and unflattened beams may be attributed to the difference in radiation beam quality ($\text{TPR}_{20,10} = 0.629$ vs $\text{TPR}_{20,10} = 0.667$ for 6 MV FFF and WFF, respectively). A more drastically effect of beam quality on the output correction factors, may be observed comparing Table 26 and 27 from TRS-483 which reports $k^{f_{clin},f_{msr}}_{Q_{clin},Qmsr}$ values for 6 MV ($\text{TPR}_{20,10} \approx 0.629$ to 0.677) and 10 MV ($\text{TPR}_{20,10} \approx 0.716$ to 0.730) photon beams. Overall, the correction factors for 10 MV are less than the correction factors for 6 MV. An unflattened beam has a softer beam than a flattened one due to more low-energy photons present on the beam[30]. The presence of low-energy photons might increase the p_{wall} and density effects [6], slightly increasing the ionization chamber's sub-response for the case of 6 MV FFF. Further research is required to understand these differences in depth.

Figure 7b shows a comparison between $k^{f_{clin},f_{msr}}_{Q_{clin},Q_{msr}}$ calculated for 6 MV WFF beams and output correction factors measured [28] or calculated [29] by other authors. These correction factors were determined using linacs different from TrueBeam STx®. An excellent agreement can be observed within 1% between all the correction factors for the studied field sizes. Even for some field sizes (2, 3 and 6 cm length size), the agreement was better than 0.5%. This agreement between independently calculated output correction factors may be caused by the fact that the IBA-CC01 ionization chamber possesses the simplest design among the detectors studied in this work. The IBA-CC01 has a single wall (the same wall is the external electrode) made of C551 plastic. It has been reported that radiation transport on thin layers (as present in many radiation detectors) might introduce differences in dose calculations performed using different Monte Carlo libraries [31].

Overall, the results of the present work shows that $k^{f_{clin},f_{msr}}_{Q_{clin},Q_{msr}}$ might be calculated using our MC linac model for 6 MV FFF beams in the context and methods of TRS-483. It is important to remark that there are no published output correction factors that were MC calculated using the TrueBeam STx® linac because of vendor restriction on linac's design as far as the authors' knowledge. The existing correction factors in TRS-483, where the TrueBeam STx® linac was used, were determined experimentally for several detectors (not used in this work) [14, 15]. Moreover, Akino et al. [32] applied TRS-483 code of practice on a multi-institutional study. It was found that after application of output correction factors there were differences up to 5% between the field factors for a 0.5 cm× 0.5 cm field size for several detectors (among them IBA-CC01 and SFD, and PTW-31016). The results of this work showed that such differences can not be attributed to $k^{f_{clin},f_{msr}}_{Q_{clin},Q_{msr}}$ at least for the detectors used in this work.

3.4. Evaluation of the latent variance of the phase spaces files generated with the MC model of the Varian TrueBeam STx® linac

Figure 8 shows dose variance as a function of $1/N_{recycl}$ and field size for 0.01 and 0.3 cm^3 voxel size. The calculated dose variance were between 0.1 to 20% for 0.01 cm^3, and 0.003 to 0.015% for 0.01 cm^3 voxel size. The difference in dose variance between voxel sizes is due to the difference in voxel volumes. A greater voxel volume allows a greater energy fluence inside the voxel, thus increasing the calculated dose's accuracy and decreasing the variance. Table 3 shows the LV as a function of field size for both voxel sizes. LV was calculated by extrapolating the linear fit to a $1/N_{recycl}$ equal to zero (N_{recycl} approaches to infinity). It can be observed that for 0.01 cm^3 voxel size, the LV had values from ∼0.2% to 0.6%, while for 0.3 cm^3 had an approximately constant value of 0.03% for all field sizes. Alhakeem et al. [23] analyzed and calculated LV values for the TrueBeam's PHSP files provided by Varian. For 6 MV beam, Alhakeem et al. found that LV values about 1% might achieve using one single PHSP file (1 from 50) for 10 cm× 10 cm field size and 0.5 cm^3 voxels. For small circular beams, LV values

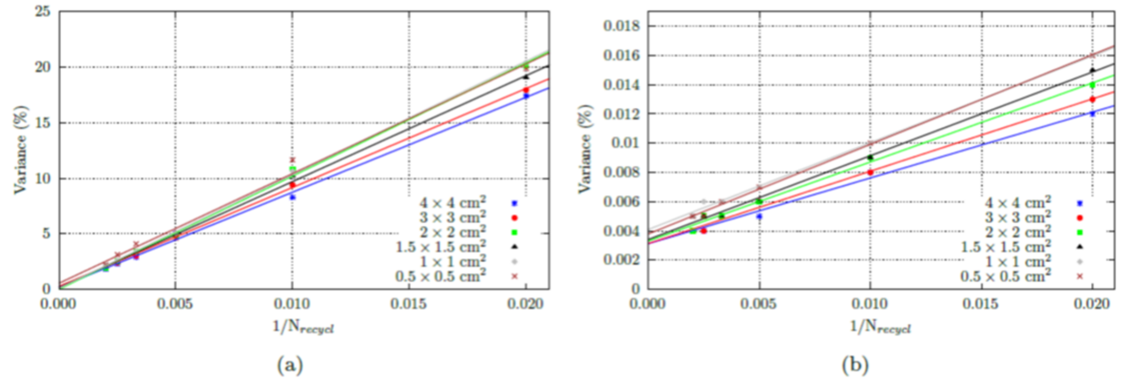

Figure 8: Latent Variance (LV) evaluation plot using a voxel with dimensions of (a) $0.01 \times 0.01 \times 0.01$ cm^3 and (b) $0.3 \times 0.3 \times 0.3$ cm^3. The PHSP used to calculate the dose variance were those obtained from the 6 MV FFF MC model of the Varian TrueBeam STx® linac developed on BEAMnrc

were 8 and 16% for 1.0 and 0.4 beam diameter, respectively. The above LV values are not adequate for calculating output correction factors, which requires at least LV values $\leq 1\%$ for small beams. These LV values can not be achieved using Varian PHSP files because of the limited particles available. The Monte Carlo linac model of the TrueBeam STx® developed in this work does not have such limitations. The particle density was about 6×10^6 cm^{-2} for all PHSP files generated with our Monte Carlo linac model for each field size used in this work. Alhakeem et al. reported particle density of $\sim 2 \times 10^3$ and $\sim 66 \times 10^3$. cm^{-2}.

		LV (%)	
	Voxel size (cm^3)	$0.01 \times 0.01 \times 0.01$	$0.3 \times 0.3 \times 0.3$
Field size (cm^2)	4×4	0.194%	0.003%
	3×3	0.267%	0.003%
	2×2	0.009%	0.003%
	1.5×1.5	0.164%	0.003%
	1×1	0.089%	0.004%
	0.5×0.5	0.547%	0.004%

Table 3: Latent variance (LV) evaluation for the 6 MV FFF PHSP obtained from the MC model of the Varian TrueBeam STx® linac developed on BEAMnrc. The voxel size represents an approximation to the size of the active volume of the detectors used in the study.

4. Conclusions

In this work, a set of correction factors $k_{Q_{clin},Q_{msr}}^{f_{clin},f_{msr}}$ were calculated using MC methods for the detectors PTW-31010, PTW-31016, IBA-CC01 and IBA-SFD using 6 MV FFF photon beams of an in-house MC model of a Varian TrueBeam STx® linac for 0.5×0.5, 1×1, 1.5×1.5, 2×2, 3×3, 4×4 and 6×6 cm^2 field sizes. It was found that the output correction factors calculated in this work fully agree with those reported by TRS-483 within $\sim 1\%$. The results of this work showed that for the detectors and field sizes studied, the generic output corrections factors from TRS-483 are adequate to be used for a TrueBeam STx®. Additionally, it was shown that the MC model of the Varian TrueBeam STx® is preferred over Varian PHSP files for output correction factor calculation because the MC linac model has low latent variance.

References

[1] S. Benedict, D. Schlesinger, S. Goetsch, B. Kavanagh, Stereotactic Radiosurgery and Stereotactic Body Radiation Therapy, Imaging in medical diagnosis and therapy, Taylor & Francis, 2014. `doi:10.1201/b16776`.

[2] S. Webb, Intensity-Modulated Radiation Therapy, Series in Medical Physics and Biomedical Engineering, CRC Press, 2015.

[3] Absorbed Dose Determination in External Beam Radiotherapy, no. 398 in Technical Reports Series, INTERNATIONAL ATOMIC ENERGY AGENCY, Vienna, 2001. `doi:10.1097/00004032-200111000-00017`.

[4] I. J. Das, G. X. Ding, A. Ahnesjö, Small fields: Nonequilibrium radiation dosimetry, Medical Physics 35 (1) (2008) 206–215. `doi:10.1118/1.2815356`.

[5] R. Alfonso, P. Andreo, R. Capote, M. S. Huq, W. Kilby, P. Kjäll, T. R. Mackie, H. Palmans, K. Rosser, J. Seuntjens, W. Ullrich, S. Vatnitsky, A new formalism for reference dosimetry of small and nonstandard fields, Medical Physics 35 (11) (2008) 5179–5186. `doi:10.1118/1.3005481`.

[6] INTERNATIONAL ATOMIC ENERGY AGENCY, Dosimetry of Small Static Fields Used in External Beam Radiotherapy, no. 483 in Technical Reports Series, INTERNATIONAL ATOMIC ENERGY AGENCY, Vienna, 2017.

[7] G. Cranmer-Sargison, S. Weston, J. A. Evans, N. P. Sidhu, D. I. Thwaites, Implementing a newly proposed Monte Carlo based small field dosimetry formalism for a comprehensive set of diode detectors, Medical Physics 38 (12) 6592–6602. `doi:10.1118/1.3658572`.

[8] G. Cranmer-Sargison, S. Weston, J. A. Evans, N. P. Sidhu, D. I. Thwaites, Monte Carlo modelling of diode detectors for small field MV photon dosimetry: detector model simplification and the sensitivity of correction factors to source parameterization, Physics in Medicine and Biology 57 (16) (2012) 5141–5153. doi:10.1088/0031-9155/57/16/5141.

[9] P. Francescon, S. Cora, N. Satariano, Calculation of for several small detectors and for two linear accelerators using Monte Carlo simulations, Medical Physics 38 (12) (2011) 6513–6527. doi:10.1118/1.3660770.

[10] D. Czarnecki, K. Zink, Monte Carlo calculated correction factors for diodes and ion chambers in small photon fields, Physics in medicine and biology 58 (2013) 2431–2444. doi:10.1088/0031-9155/58/8/2431.

[11] H. Benmakhlouf, J. Sempau, P. Andreo, Output correction factors for nine small field detectors in 6 MV radiation therapy photon beams: A penelope Monte Carlo study, Medical Physics 41 (4) (2014) 041711. doi:10.1118/1.4868695.

[12] J. M. Lárraga-Gutiérrez, P. Ballesteros-Zebadúa, M. Rodríguez-Ponce, O. A. García-Garduño, O. O. G. de la Cruz, Properties of a commercial PTW-60019 synthetic diamond detector for the dosimetry of small radiotherapy beams, Physics in Medicine and Biology 60 (2) (2015) 905–924. doi:10.1088/0031-9155/60/2/905.

[13] J. M. Lárraga-Gutiérrez, Experimental determination of field factors ($\Omega^{f_{\mathrm{clin}},f_{\mathrm{msr}}}_{Q_{\mathrm{clin}},Q_{\mathrm{msr}}}$) for small radiotherapy beams using the daisy chain correction method, Physics in Medicine & Biology 60 (15) (2015) 5813. doi:10.1088/0031-9155/60/15/5813.

[14] S. Tanny, N. Sperling, E. I. Parsai, Correction factor measurements for multiple detectors used in small field dosimetry on the varian edge radiosurgery system, Medical Physics 42 (9) (2015) 5370–5376. doi:10.1118/1.4928602.

[15] T. S. A. Underwood, B. C. Rowland, R. Ferrand, L. Vieillevigne, Application of the exradin w1 scintillator to determine Ediode 60017 and microDiamond 60019 correction factors for relative dosimetry within small MV and FFF fields, Physics in Medicine and Biology 60 (17) (2015) 6669–6683. doi:10.1088/0031-9155/60/17/6669.

[16] M. Rodriguez, J. Sempau, A. Fogliata, L. Cozzi, W. Sauerwein, L. Brualla, A geometrical model for the Monte Carlo simulation of the TrueBeam linac, Physics in Medicine and Biology 60 (11) (2015) N219–N229. doi:10.1088/0031-9155/60/11/n219.

[17] S. S. Almberg, J. Frengen, A. Kylling, T. Lindmo, Monte Carlo linear accelerator simulation of megavoltage photon beams: Independent determination of initial beam parameters, Medical Physics 39 (1) 40–47. doi:10.1118/1.3668315.

[18] L. L. W. Wang, K. Leszczynski, Estimation of the focal spot size and shape for a medical linear accelerator by Monte Carlo simulation, Medical Physics 34 (2) (2007) 485–488. doi:10.1118/1.2426407.

[19] B. Fraass, K. Doppke, M. Hunt, G. Kutcher, G. Starkschall, R. Stern, J. Van Dyke, American association of physicists in medicine radiation therapy committee task group 53: Quality assurance for clinical radiotherapy treatment planning, Medical Physics 25 (10) (1998) 1773–1829. doi:10.1118/1.598373.

[20] J. C. for Guides in Metrology, Jcgm 100: Evaluation of measurement data - guide to the expression of uncertainty in measurement, Tech. rep., JCGM (2008).

[21] J. Wulff, K. Zink, I. Kawrakow, Efficiency improvements for ion chamber calculations in high energy photon beams, Medical physics 35 (2008) 1328–36. doi:10.1118/1.2874554.

[22] J. Sempau, A. Sanchez-Reyes, F. Salvat, H. Tahar, S. Jiang, J. Fernández-Varea, Monte Carlo simulation of electron beams from an accelerator head using PENELOPE, Physics in medicine and biology 46 (2001) 1163–86. doi:10.1088/0031-9155/46/4/318.

[23] E. Alhakeem, S. Zavgorodni, Evaluation of latent variances in Monte Carlo dose calculations with Varian TrueBeam photon phase-spaces used as a particle source, Physics in Medicine and Biology 63 (1) (2018) 01NT03. doi:10.1088/1361-6560/aa9f39.

[24] M. López-Sánchez, M. Pérez-Fernández, J. M. Fandiño, A. Teijeiro, V. Luna-Vega, N. Gómez-Fernández, F. Gómez, D. M. González-Castaño, An egs monte carlo model for varian truebeam treatment units: Commissioning and experimental validation of source parameters, Physica Medica 64 (2019) 81 – 88. doi:https://doi.org/10.1016/j.ejmp.2019.06.017.

[25] D. Sawkey, M. Constantin, S. Mansfield, J. Star-Lack, A. Rodrigues, Q. Wu, M. Svatos, Su-e-t-553: Measurement of incident electron spots on truebeam, Medical Physics 40 (2013) 332–332. doi:10.1118/1.4814982.

[26] X. Li, M. Soubra, J. Szanto, L. H Gerig, Lateral electron equilibrium and electron contamination in measurements of head-scatter factors using miniphantoms and brass caps, Medical physics 22 (1995) 1167–70. doi:10.1118/1.597508.

[27] A. Scott, S. Kumar, A. Nahum, J. Fenwick, Characterizing the influence of detector density on dosimeter response in non-equilibrium small photon fields, Physics in Medicine and Biology 57 (2012) 4461–4476. doi:10.1088/0031-9155/57/14/4461.

[28] G. Azangwe, P. Grochowska, D. Georg, J. Izewska, J. Hopfgartner, W. Lechner, C. E. Andersen, A. R. Beierholm, J. Helt-Hansen, H. Mizuno, A. Fukumura, K. Yajima, C. Gouldstone, P. Sharpe,

A. Meghzifene, H. Palmans, Detector to detector corrections: A comprehensive experimental study of detector specific correction factors for beam output measurements for small radiotherapy beams, Medical Physics 41 (7) (2014) 072103. arXiv:https://aapm.onlinelibrary.wiley.com/doi/pdf/10.1118/1.4883795, doi:10.1118/1.4883795.
URL https://aapm.onlinelibrary.wiley.com/doi/abs/10.1118/1.4883795

[29] H. Benmakhlouf, J. Sempau, P. Andreo, Output correction factors for nine small field detectors in 6 mv radiation therapy photon beams: A penelope monte carlo study, Medical Physics 41 (4) (2014) 041711. arXiv:https://aapm.onlinelibrary.wiley.com/doi/pdf/10.1118/1.4868695, doi:10.1118/1.4868695.
URL https://aapm.onlinelibrary.wiley.com/doi/abs/10.1118/1.4868695

[30] R. D. Foster, M. P. Speiser, T. D. Solberg, Commissioning and verification of the collapsed cone convolution superposition algorithm for sbrt delivery using flattening filter-free beams, Journal of Applied Clinical Medical Physics 15 (2) (2014) 39–49. arXiv:https://aapm.onlinelibrary.wiley.com/doi/pdf/10.1120/jacmp.v15i2.4631, doi:10.1120/jacmp.v15i2.4631.
URL https://aapm.onlinelibrary.wiley.com/doi/abs/10.1120/jacmp.v15i2.4631

[31] V. F. Casssola, G. Hoff, Comparison between geant4 and egsnrc of dosimetric quantities and spectra simulation for electrons beam, in: 2011 IEEE Nuclear Science Symposium Conference Record, 2011, pp. 1398–1400. doi:10.1109/NSSMIC.2011.6154626.

[32] Y. Akino, H. Mizuno, M. Isono, Y. Tanaka, N. Masai, T. Yamamoto, Small-field dosimetry of truebeamtm flattened and flattening filter-free beams: A multi-institutional analysis, Journal of Applied Clinical Medical Physics 21 (1) (2020) 78–87. arXiv:https://aapm.onlinelibrary.wiley.com/doi/pdf/10.1002/acm2.12791, doi:10.1002/acm2.12791.
URL https://aapm.onlinelibrary.wiley.com/doi/abs/10.1002/acm2.12791